Antioxidant administration attenuates mechanical ventilation-induced rat diaphragm muscle atrophy independent of protein kinase B (PKB–Akt) signalling

J. M. McClung, A. N. Kavazis, M. A. Whidden, K. C. DeRuisseau, D. J. Falk, D. S. Criswell and S. K. Powers

Department of Applied Physiology and Kinesiology, University of Florida, Gainesville, FL 32611, USA

Oxidative stress promotes controlled mechanical ventilation (MV)-induced diaphragmatic atrophy. Nonetheless, the signalling pathways responsible for oxidative stress-induced muscle atrophy remain unknown. We tested the hypothesis that oxidative stress down-regulates insulin-like growth factor-1–phosphotidylinositol 3-kinase–protein kinase B serine threonine kinase (IGF-1–PI3K–Akt) signalling and activates the forkhead box O (FoxO) class of transcription factors in diaphragm fibres during MV-induced diaphragm inactivity. Sprague–Dawley rats were randomly assigned to one of five experimental groups: (1) control (Con), (2) 6 h of MV, (3) 6 h of MV with infusion of the antioxidant Trolox, (4) 18 h of MV, (5) 18 h of MV with Trolox. Following 6 h and 18 h of MV, diaphragmatic Akt activation decreased in parallel with increased nuclear localization and transcriptional activation of FoxO1 and decreased nuclear localization of FoxO3 and FoxO4, culminating in increased expression of the muscle-specific ubiquitin ligases, muscle atrophy factor (*MAFbx*) and muscle ring finger-1 (*MuRF-1*). Interestingly, following 18 h of MV, antioxidant administration was associated with attenuation of MV-induced atrophy in type I, type IIa and type IIb/IIx myofibres. Collectively, these data reveal that the antioxidant Trolox attenuates MV-induced diaphragmatic atrophy independent of alterations in Akt regulation of FoxO transcription factors and expression of *MAFbx* or *MuRF-1*. Further, these results also indicate that differential regulation of diaphragmatic IGF-1–PI3K–Akt signalling exists during the early and late stages of MV.

(Resubmitted 20 July 2007; accepted after revision 27 September 2007; first published online 4 October 2007)
Corresponding author J. M. McClung: Department of Applied Physiology and Kinesiology, University of Florida, Room 25 Florida Gym, Gainesville, FL 32611, USA. Email: mmcclung@hhp.ufl.edu

Recent studies indicate that mechanical ventilation (MV), which is used to maintain alveolar ventilation in patients incapable of sustaining adequate ventilation (i.e. during respiratory failure), results in a rapid onset of diaphragmatic fibre atrophy and contractile dysfunction (Le Bourdelles *et al.* 1994; Shanely *et al.* 2002; Gayan-Ramirez *et al.* 2003; Levine *et al.* 2006). Interestingly, the proteolysis and decreased protein synthesis (Shanely *et al.* 2003, 2004; DeRuisseau *et al.* 2005*a*) that occur during MV-induced diaphragmatic atrophy are more rapid than the rates observed in locomotor muscles subjected to disuse (Thomason *et al.* 1989; McClung *et al.* 2007). These facts suggest that the signalling associated with diaphragm myofibre atrophy during MV may involve different and/or accelerated mechanisms compared to models of postural muscle atrophy.

Signalling initiated by the growth factor ligand insulin-like growth factor-1 (IGF-1) exerts a critical influence on skeletal muscle myofibre size (Kandarian & Stevenson, 2002; Stitt *et al.* 2004; Glass, 2005; Kandarian & Jackman, 2006). IGF-1 binding results in the phosphorylation of the p85 regulatory subunit of phosphatidylinositol 3 kinase (PI3K) and subsequent activation of phosphoinositide-dependent kinase-1 (PDK1) and/or the serine/threonine kinase protein kinase B (PKB–Akt) (reviewed in Kandarian & Jackman, 2006). Recent evidence demonstrates that disuse-induced deactivation of components of this protein synthetic signalling pathway results in the removal of regulatory influences mediating proteolysis and proteolytic gene expression (Stitt *et al.* 2004; Latres *et al.* 2005). In this regard, Akt exerts a repressor influence on the activation of the forkhead box O (FoxO) class of transcription factors, which includes FKHR (FoxO1), FKHRL1 (FoxO3) and AFX (FoxO4) (Stitt *et al.* 2004; Fig. 1). This is of paramount importance in skeletal muscle due to the role of FoxOs in the regulation of the muscle-specific ubiquitin

 DOI: 10.1113/jphysiol.2007.141119

ligases muscle atrophy factor (*MAFbx* or atrogin) and muscle ring finger-1 (*MuRF-1*) (Sandri *et al.* 2004; Stitt *et al.* 2004).

Previous work in our laboratory indicates that unloading the diaphragm via prolonged MV results in increased proteolysis in this key inspiratory muscle (Shanely *et al.* 2003, 2004; DeRuisseau *et al.* 2005*a*). Based on previous reports investigating IGF-1–PI3K–Akt's signalling influence in atrophying skeletal muscle (Sandri *et al.* 2004; Stitt *et al.* 2004), we hypothesized that MV-induced disuse in the diaphragm would result in down-regulation of the IGF-1–PI3K–Akt pathway resulting in increased FoxO activation. Moreover, our research reveals that alleviation of MV-induced oxidative stress results in the attenuation of diaphragmatic proteolysis and reduced activity of the 20S proteasome (Betters *et al.* 2004). Nonetheless, it is unknown whether the catabolic influence of oxidative stress impacts IGF-1–PI3K–Akt signalling during MV. Based upon our prior work, we further hypothesized that oxidative stress induced alterations in IGF-1–PI3K–Akt signalling to FoxO transcription factors is a critical mechanism for the development of muscle atrophy in the diaphragm during MV. Our results support the hypothesis of an initial decline in IGF-1–PI3K–Akt signalling. Importantly, our data also reveal that the alleviation of oxidative injury to the diaphragm attenuates atrophy induced by MV independent of Akt's influence on FoxO regulation of *MAFbx* and *MuRF-1* ubiquitin ligase gene expression.

Methods

Experimental design

Adult (6 months old) female Sprague–Dawley rats were randomly assigned to an acutely anaesthetized control group (Con; $n = 6$); (2) a 6 h controlled mechanical ventilation (MV) group (6 h MV; $n = 6$); (3) a 6 h MV group with exogenous administration of the antioxidant Trolox ($n = 6$); (4) an 18 h MV group ($n = 6$); and (5) an 18 h MV group with exogenous administration of the antioxidant Trolox ($n = 6$). Controlled mechanical ventilation for a 6 h time frame was chosen due to previous experiments demonstrating this length of MV as sufficient to induce the onset of diaphragmatic oxidative stress without significant alterations to myofibre cross-sectional area (Zergeroglu *et al.* 2003; McClung *et al.* 2007). Controlled mechanical ventilation for an 18 h time frame was chosen due to previous experiments demonstrating this length of MV as sufficient for the advanced progression of significant diaphragm atrophy, contractile dysfunction, proteolysis and oxidative stress (Powers *et al.* 2002; Zergeroglu *et al.* 2003; Betters *et al.* 2004). At the completion of the experimental protocol,

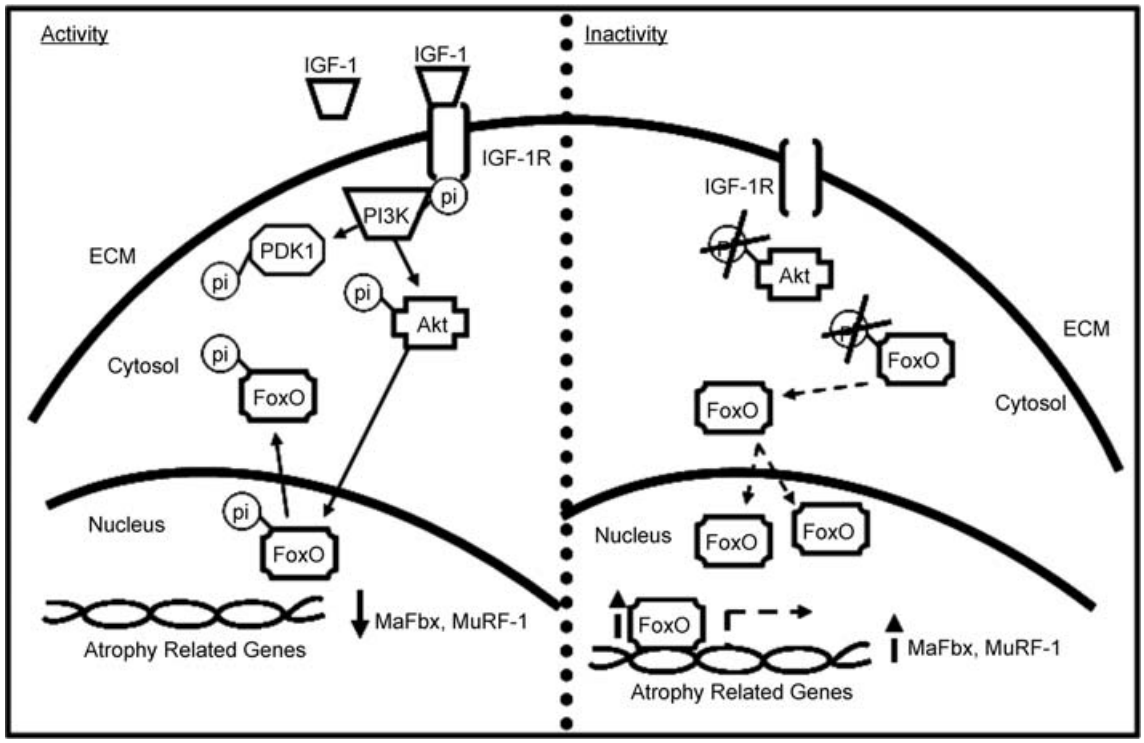

Figure 1. Simplified schematic diagram of protein kinase B (PKB–Akt) signalling pathways shown to be involved in inactivity atrophy
Involvement of the pathways shown here is discussed in the Introduction. Signalling represented is one likely component (Sandri *et al.* 2004; Stitt *et al.* 2004) of the overall complex signalling pathways involved in atrophy.

anaesthetized animals were euthanized by thoracotomy involving diaphragm and heart excision. All experiments were conducted in accordance with the policies contained in the *Guide for the Care and Use of Laboratory Animals* and were approved by the University of Florida Animal Care and Use Committee.

Acutely anaesthetized controls

Control animals were subjected to an acute plane of surgical anaesthesia with an I.P. injection of sodium pentobarbital (60 mg (kg body weight)$^{-1}$). Segments of the costal diaphragm were then removed, rapidly frozen in liquid nitrogen and stored at −80°C for subsequent biochemical and molecular analyses. The efficacy of acutely anaesthetized controls was determined by previous work demonstrating that: (1) sodium pentobarbital does not negatively impact diaphragm contractile function nor promote muscle atrophy (Le Bourdelles *et al.* 1994); (2) spontaneously breathing control groups do not experience increased diaphragmatic oxidative stress or diaphragm myofibre atrophy (Shanely *et al.* 2002; Zergeroglu *et al.* 2003); and (3) inactivity of the postural plantaris muscle during MV does not induce muscle atrophy (McClung *et al.* 2007).

Controlled mechanical ventilation

All surgical procedures were performed using aseptic techniques (Powers *et al.* 2002; Shanely *et al.* 2002; Criswell *et al.* 2003; Zergeroglu *et al.* 2003). Animals randomly selected for MV were anaesthetized with an I.P. injection of sodium pentobarbital (60 mg (kg body weight)$^{-1}$). After reaching a surgical plane of anaesthesia, the animals were tracheostomized and mechanically ventilated using a volume-driven small animal ventilator (Harvard Apparatus, Cambridge, MA, USA). The ventilator delivered all breaths; hence, this mode of ventilation (i.e. controlled MV) results in complete diaphragmatic inactivity (Powers *et al.* 2002). The tidal volume was established at approximately 0.55 ml (100 g body weight)$^{-1}$ with a respiratory rate of 80 breaths min^{-1}. This respiratory rate was selected to mimic the breathing frequency of adult rats at rest. Additionally, positive end-expiratory pressure of 1 cmH_2O was used throughout the protocol. An arterial catheter was inserted into the carotid artery for constant measurement of blood pressure. Moreover arterial blood samples (100 μl per sample) were removed during the first and last hour of MV and analysed for arterial P_{CO_2}, P_{O_2} and pH using a blood gas analyser (model 1610, Instrumentation Laboratories Company, Lexington, MA, USA). Anaesthesia was maintained over the entire period of MV by continuous infusion of sodium pentobarbital (10 mg (kg body weight)$^{-1}$ h^{-1}) via a venous catheter that was inserted into the jugular vein. Body temperature was maintained at 37–37.5°C (±0.5°C) using a re-circulating heating blanket. Additionally, heart rate and electrical activity of the heart were monitored via a lead II ECG using needle electrodes placed subcutaneously.

Body fluid homeostasis was maintained via the administration of 2.0 ml kg^{-1} h^{-1} intravenous electrolyte solution. Continuing care during MV included expressing the bladder, removing airway mucus, lubricating the eyes, rotating the animal and passive movement of the limbs. This care was maintained throughout the experimental period at hourly intervals. Finally, intramuscular injections of glycopyrrolate (0.04 mg kg^{-1} (2 h)$^{-1}$) were employed to reduce airway secretions during MV. Upon completion of MV, segments of the costal diaphragm were removed, rapidly frozen in liquid nitrogen and stored at −80°C for subsequent biochemical and molecular analysis.

Trolox administration

Exogenous administration of the water-soluble antioxidant Trolox ((±)-6-hydroxy-2,5,7,8-tetramethylchromane-2-carboxylic acid; Sigma Aldrich) was performed as previously described (Betters *et al.* 2004). Trolox is a peroxyl radical scavenger that has previously been shown to rapidly penetrate cell membranes and be more effective as an antioxidant than its parent compound, vitamin E (Sagach *et al.* 2002). The primary protective effects of Trolox appears to be based on its capacity to inhibit membrane lipid peroxidations and protein carbonylation (Wu *et al.* 1990; Bizzozero *et al.* 2007). Briefly, a priming dose of Trolox (20 mg kg^{-1}) was infused over a 5 min period, 20 min prior to the start of MV. During MV, Trolox or saline vehicle was infused continuously at a rate of 4 mg kg^{-1} h^{-1} for the entirety of the ventilation treatment. Eighteen hours of Trolox pretreatment was also administered to acutely anaesthetized control animals ($n = 5$) to determine the independent effects of Trolox on non-mechanically ventilated diaphragm skeletal muscle.

Total glutathione and protein carbonyls

Total glutathione (GSH) and protein carbonyls were analysed as indicators of oxidative stress. Total glutathione was measured using a commercially available spectrophotometric kit (Cayman Chemical, Ann Arbor, MI, USA). Briefly, 40–50 mg costal diaphragm was analysed for GSH according to manufacturer's recommendations. Sample protein content was assayed using the Bradford method (Sigma, St Louis, MO, USA). Protein carbonyls were measured in 40–50 mg total costal diaphragm muscle using a commercially available

enzyme-lined immunosorbent assay (ELISA) (Biocell PC Test, Northwest Life Science Specialties, LLC, Vancouver, WA, USA) according to the manufacturer's instructions.

Myofibre cross-sectional area and morphological analyses

Serial sections from frozen diaphragm samples were cut at 10 μm using a cryotome (Shandon Inc., Pittsburgh, PA, USA). Sections for cross-sectional area analysis were then dried at room temperature for 30 min and incubated in a PBS solution containing 0.5% Triton X-100. Sections were then rinsed in PBS and simultaneously exposed to primary antibodies specific to dystrophin protein (rabbit host, Lab Vision Corporation), myosin heavy chain type I (mouse host, immunoglobulin M (IgM) isotype, Developmental Studies Hybridoma Bank, Iowa City, IA, USA; Jergovic *et al.* 2001), and MHC type IIa (mouse host, immunoglobulin G (IgG) isotype, a kind gift from Takao Sugiura, Laboratory of Biomechanics and Physiology, Faculty of Liberal Arts, Yamaguchi University, Yamaguchi, Japan; Ausoni *et al.* 1990), in a dark humid chamber at room temperature for 1 h. Sections were subsequently rinsed 3 times in PBS and exposed to rhodamine red anti-rabbit secondary antibody (Molecular Probes, Eugene, OR, USA), Alexa Fluro 350 goat anti-mouse IgM isotype-specific secondary antibody (Molecular Probes), and Alexa Fluro 488 goat anti-mouse IgG isotype-specific secondary antibody (Molecular Probes) diluted in PBS containing 0.5% Pierce Super Blocker (57535, Pierce) in a dark humid chamber at room temperature for 1 h. Sections were then washed in PBS and mounted with Vectashield (Vector Laboratories, Burlingame, CA, USA). After mounting, slides were coverslipped and sealed for viewing via an inverted fluorescence microscope (Carl Zeiss Axiovert 200). Fibre typing utilizing this method allows for the individual visualization of the myofibre membrane protein dystrophin using the rhodamine filter set (red), type I myosin using the DAPI filter set (blue), type IIa myosin using the FITC filter set (green), and type IIb/IIx (non-stained/black) myofibres. Images were obtained at a $\times$10 magnification, and approximately 250 myofibres, a number chosen by determination of no additional change in standard deviation, were analysed for myofibre cross-sectional area (μm^2) using Scion Image software (Scion Technologies, Frederick, MD, USA) by a blinded investigator.

Fractionation of cellular homogenates

Cytosolic and nuclear protein fractions were obtained from costal segments of the diaphragm as previously described (Siu & Alway, 2005). Briefly, muscle was homogenized at 4°C using a glass on glass homogenizer in ice-cold cell lysis buffer (10 mM NaCl, 1.5 mM $MgCl_2$, 20 mM Hepes, pH 7.4, 20% glycerol, 0.1% Triton X-100, and 1 mM DTT). Following a brief centrifugation (3 min) at 880 *g* at 4°C to pellet nuclei and cellular debris, supernatants were subjected to three subsequent bouts of centrifugation (3500 *g* at 4°C for 5 min each) to remove residual nuclei. The supernatant then received a protease inhibitor cocktail and was stored as nuclei-free total cytosolic protein fraction. The remaining nuclear pellets were then washed 3 times in lysis buffer, re-suspended in 300 μl of lysis buffer with 41.5 μl of 5 M NaCl and protease inhibitor cocktail, and rotated at 4°C for 1 h to lyse the nuclei. Lysed nuclei were then spun at 21 900 *g* for 15 min at 4°C, the supernatants were collected and stored as cytosol-free nuclear protein extracts at −80°C for Western blotting.

Western blotting

Cytosolic and nuclear protein extracts were assayed using the Bradford method (Sigma). Proteins, 100 μg from both fractions, were then separated by polyacrylamide gel electrophoresis via 4–15% gradient and transferred to nitrocellulose membranes (100 V for 3 h at 4°C). The resulting membrane was then stained with Ponceau S and visually inspected for equal protein loading and transfer. Images of each Ponceau S-stained membrane were analysed using computerized image analysis (Scion Image) to further verify equal loading and transfer between lanes (data not shown). Membranes were then washed and blocked in PBS–Tween buffer containing 5% skimmed milk and 0.05% Tween for 2 h and subsequently incubated initially with anti-histone H2B (1 : 2000 dilution; Upstate, Lake Placid, NY, USA) and anti-CuZnSOD (anti-copper zinc superoxide dismutase; 1 : 500 dilution, Santa Cruz, CA, USA) primary antibodies to verify purity of nuclear and cytosolic fractions, respectively (Fig. 4*A*). Subsequent membranes were washed, blocked, and incubated with antibodies against p85 PI3K, phospho (Tyr) p85 PI3K, PDK1, phospho (Ser-241) PDK1, Akt, phospho (Ser-473) Akt, FKHR (FoxO1), phospho (Ser-256) FKHR (FoxO1), FKHRL1 (FoxO3), phospho (Thr 24) FKHRL1 (FoxO3), AFX (FoxO4), and phospho (Ser-193) AFX (FoxO4), all purchased from Cell Signalling Technology (Carlsbad, CA, USA). Primary antibodies were diluted 1 : 1000 or 1 : 200 (FoxO1, FoxO3, FoxO4 total and phosphorylated antibodies) in blocking buffer and applied to the membranes with gentle rocking overnight at 4°C. Membranes were then incubated with horseradish peroxidase-antibody conjugate (1 : 2000) directed against the primary antibody for 2 h. Membranes were then treated with chemiluminescent reagents (luminol and enhancer; ECL Plus, Amersham Biosciences, Piscataway, NJ, USA) and exposed to light-sensitive film. Film

images were captured and subsequently analysed using computerized image analysis (Scion Image, Frederick, MD, USA). Values for PI3K, PDK1, cytosolic Akt, and nuclear Akt proteins are presented as the percentages of total phosphorylated protein abundances as an indicator of activity.

FKHR transcriptional activation

FKHR (FoxO1) transcriptional activation was analysed in isolated diaphragm nuclear extracts using a commercially available transcription factor assay kit (TransAM, Active Motif; Carlsbad, CA, USA) according to the manufacturer's instructions.

RNA isolation and cDNA synthesis

Total RNA was isolated from muscle tissue using TRIzol Reagent (Life Technologies, Carlsbad, CA, USA), according to the manufacturer's instructions. Total RNA (5 μg) was then reverse transcribed using the Superscript III First-Strand Synthesis System for RT-PCR (Life Technologies) using oligo(dT)20 primers and the protocol outlined by the manufacturer.

Real-time polymerase chain reaction

One microlitre of cDNA was added to a 25 μl PCR reaction for real-time PCR using Taqman chemistry and the ABI Prism 7000 Sequence Detection System (ABI, Foster City, CA, USA). Relative quantification of gene expression was performed using the comparative computed tomography method (ABI, User Bulletin no. 2). This method uses a single sample, the calibrator sample (*β-glucuronidase*; GenBank NM_Y00717, NM_M13962), for comparison of every unknown sample's gene expression. $\Delta\Delta$CT (ΔCT(calibrator) $-$ ΔCT(sample)) was then calculated for each sample and relative quantification was calculated as $2\Delta\Delta$CT. *β-Glucuronidase*, a lysosomal glycoside hydrolase, was chosen as the reference gene based on initial experiments and previous work showing unchanged expression with our experimental manipulations (DeRuisseau *et al.* 2005*b*,*c*). Fivefold dilution curves were assayed on selected samples to confirm the validity of this quantification method for each gene. *MAFbx* (GenBank NM_AY059628) and *MuRF-1* (GenBank NM_AY059627, NM_BC061824) mRNA transcripts were assayed using predesigned rat primer and probe sequences commercially available from Applied Biosystems (Assays-on-Demand).

Statistical design

Preliminary studies of the potential effects of Trolox treatment on the diaphragm were analysed using independent *t* tests. Where no significant effects occurred in treatment controls due to Trolox pretreatment respective groups were pooled. All other comparisons between groups for each dependent variable measured were made by one-way analysis of variance (ANOVA). When significant differences were observed, a Tukey HSD (honestly significantly different) test was implemented *post hoc*. Significance was established at $P < 0.05$.

Results

Systemic and biological response to MV

Initial and final body weights of the animals did not differ ($P > 0.05$) between treatment groups (data not shown). Cardiovascular dynamics during MV was monitored via measurement of both heart rate and systolic blood pressure. Heart rate (361 ± 16 beats min^{-1}) and mean blood pressure (88 ± 13 mmHg) homeostasis were maintained during MV across all treatment groups. Blood gas homeostasis and pH (data not shown) were maintained within physiological levels during the experiment as reported previously (Powers *et al.* 2002; Shanely *et al.* 2002; Criswell *et al.* 2003; Zergeroglu *et al.* 2003).

Analysis of Trolox-pretreated control animals

The experimental design of the present study included a preliminary analysis of Trolox administration on diaphragm myofibre cross-sectional area and PKB signalling. Eighteen hours of Trolox pretreatment did not alter type I (1864 ± 267 μm^2), type IIa (1799 ± 154 μm^2), or type IIb/IIx (3701 ± 456 μm^2) myofibre cross-sectional area from non-treated control values. No significant differences were determined for nuclear and cytosolic total and phosphorylated Akt proteins; cytosolic phosphorylated FoxO1, FoxO3, or FoxO4 proteins; or nuclear total FoxO1, FoxO3 or FoxO4 proteins (data not shown). Control data were therefore combined for all further analysis.

Oxidative stress

The development of MV-induced diaphragmatic oxidative stress and the efficacy of Trolox administration as an antioxidant were determined by measuring total GSH and protein carbonyl formation. Total GSH (mmol (mg tissue wet weight)$^{-1}$; Table 1) decreased from control values with 6 and 18 h of MV. Trolox administration did not attenuate the ventilation-induced decrease at 6 or 18 h. Protein carbonyls (nmol (mg tissue wet weight)$^{-1}$) increased with 6 and 18 h of MV but were returned to control values with Trolox administration at both time-points (Table 1).

Table 1. Diaphragm total glutathione (GSH) and protein carbonyl formation with mechanical ventilation and ventilation with Trolox administration

Treatment	GSH (mmol (mg tissue wet wt)$^{-1}$)	Protein carbonyls (nmol (mg tissue wet wt)$^{-1}$)
Con	0.64 ± 0.04	0.55 ± 0.04
6 h MV	0.54 ± 0.03*	0.87 ± 0.13*
6 h MVT	0.49 ± 0.03*	0.62 ± 0.07†
18 h MV	0.37 ± 0.02*†‡	0.84 ± 0.07*‡
18 h MVT	0.34 ± 0.02*†‡	0.50 ± 0.05†κ

Control (Con), 6 h controlled mechanical ventilation (6 h MV), 6 h controlled mechanical ventilation with Trolox antioxidant administration (6 h MVT), 18 h controlled mechanical ventilation (18 h MV), and 18 h controlled mechanical ventilation with Trolox administration (18 h MVT) treatment groups. Values are means ± S.E.M. * Significantly ($P < 0.05$) different from Con. † Significantly different from 6 h MV. ‡ Significantly different from 6 h MVT. κ Significantly different from 18 h MV.

Fibre mean cross-sectional areas (CSAs)

Myofibre cross-sectional area was determined for individual fibre types in cross-sections obtained from treatment diaphragms (Fig. 2*A*). There was no effect of 6 h-controlled mechanical ventilation or 6 h ventilation with Trolox administration on type I, type IIa, and type IIb/IIx diaphragm myofibre CSA. Controlled mechanical ventilation for 18 h resulted in significant atrophy of type I, type IIa, and type IIb/IIx diaphragm myofibres (Fig. 2*B*). Importantly Trolox administration attenuated atrophy in all diaphragm myofibre types during 18 h of MV (Fig. 2*B*).

Receptor-linked cytosolic insulin signalling

Signalling through the PI3K–Akt pathway prevents expression of muscle atrophy-induced ubiquitin ligases (Stitt *et al.* 2004). The percentage of phosphorylated

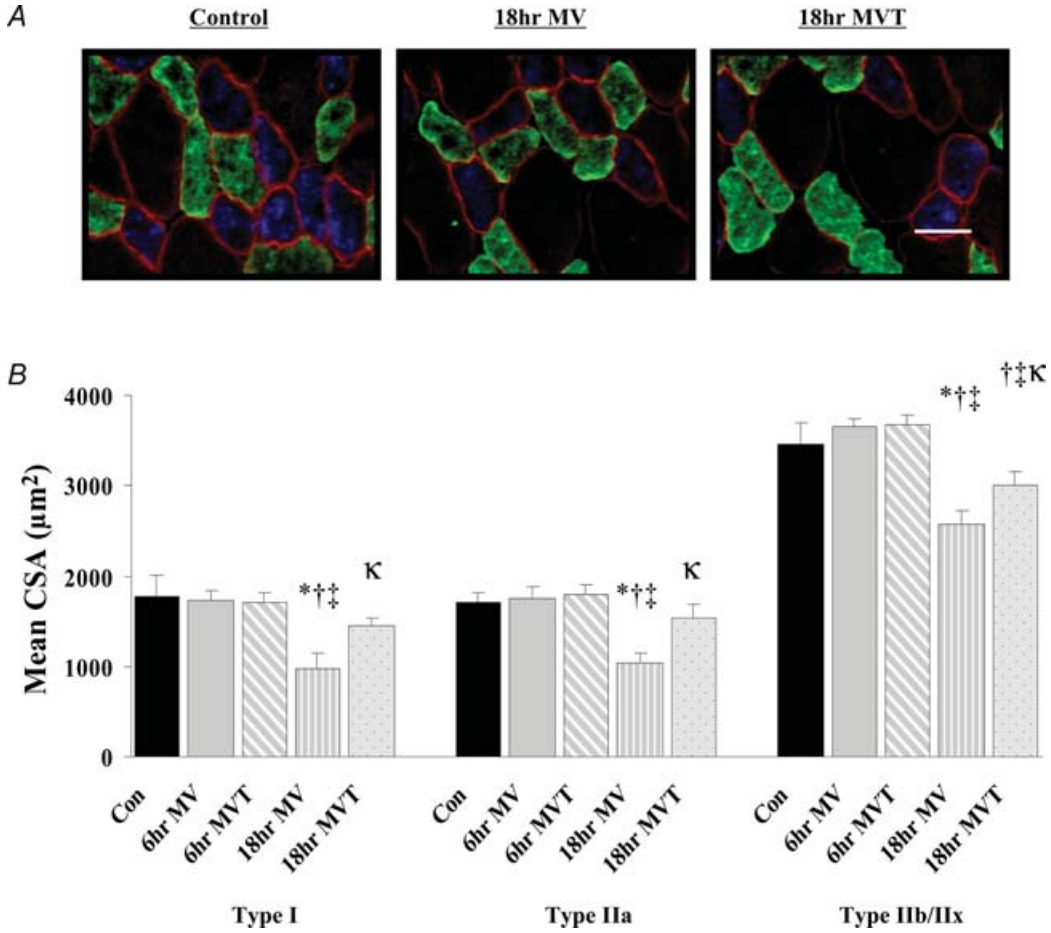

Figure 2. Fibre cross-sectional area (CSA) in diaphragm skeletal muscle myofibres expressing myosin heavy chain (MHC) I (Type I), MHC IIa (Type IIa) and MHC IIb/IIx (Type IIb/IIx)
A, representative fluorescence staining of MHC I (DAPI filter/blue), MHC IIa (FITC filter/green), and dystrophin (rhodamine filter/red) proteins in diaphragm from control (Con), 18 h mechanical ventilation (18 h MV) and 18 h mechanical ventilation with Trolox antioxidant administration (18 h MVT). *B*, mean cross-sectional area (CSA, μm^2) of type I, type IIa, and type IIb/IIx diaphragm skeletal muscle myofibres. Scale bar, 30 μm. Values are means ± S.E.M. * Significantly ($P < 0.05$) different from control values. † Significantly ($P < 0.05$) different from 6 h MV values. ‡ Significantly ($P < 0.05$) different from 6 h MVT values. κ Significantly ($P < 0.05$) different from 18 h MV values.

PI3K was not altered by mechanical ventilation or ventilation with Trolox administration (Fig. 3*A* and *B*). The percentage of phosphorylated PDK1 was also not altered by mechanical ventilation or ventilation with Trolox administration (Fig. 3*A* and *C*).

Cytosolic and nuclear insulin signalling

Akt functions in both cytosolic signalling and nuclear transcriptional regulation in eukaryotic cells (Matsuzaki *et al.* 2003; Furukawa-Hibi *et al.* 2005). Therefore, we analysed both cytosolic and nuclear compartmentalization of Akt protein during MV (Fig. 4*B*). Alterations in the phosphorylation and/or total expression of cytosolic Akt resulted in a decreased percentage of total phosphorylated (Ser-473) Akt with 18 h of MV (Fig. 4*C*). In contrast, alterations in the phosphorylation and/or total expression of nuclear Akt phosphorylation (Ser-473; Fig. 4*D*) and total nuclear Akt protein resulted in a decreased percentage of total nuclear phosphorylated Akt with 18 h of MV.

Forkhead class of transcription factors (FoxOs): cellular protein localization/phosphorylation

The FoxO class of transcription factors has recently garnered much attention for its roles in transcriptional regulation of the muscle-specific ubiquitin ligases *MAFbx* and *MuRF-1* (Bodine *et al.* 2001; Sandri *et al.* 2004; Stitt *et al.* 2004; Glass, 2005). Particularly, the activation of this class of transcription factors relies on its dephosphorylation in the cytosol and translocation to the nucleus (Stitt *et al.* 2004). Therefore, we chose to analyse both the cytosolic phosphorylation state and total nuclear abundance of FoxO1, FoxO3 and FoxO4 proteins (Fig. 5*A*). Western analysis revealed low, but detectable, phosphorylated FoxO1, FoxO3 and FoxO4 protein in the cytosol, with FoxO4 levels representing the phosphorylated protein of least abundance. Cytosolic phosphorylation of both FoxO1 (Ser-256; Fig. 5*B*) and FoxO4 (Ser-193; Fig. 5*D*) proteins decreased with both 6 and 18 h of MV. There was no effect, however, of 6 or 18 h of MV on the cytosolic phosphorylation (Thr-32) of FoxO3 (Fig. 5*C*). Nuclear abundance of FoxO1 (Fig. 5*E*) protein increased with 6 and 18 h of MV. However, there were decreases in nuclear abundances of both FoxO3 (Fig. 5*F*) and FoxO4 (Fig. 5*G*) with both 6 and 18 h of MV.

FKHR transcriptional activation and muscle-specific ubiquitin ligase gene expression

The DNA binding of FoxO1 was analysed in an attempt to determine whether increases in the nuclear localization of this protein corresponded with increases in its activity as a transcriptional coactivator. Binding of FoxO1 nuclear protein to a corresponding oligonucleotide sequence increased with both 6 and 18 h of MV and was unaffected by Trolox administration (Fig. 6*A*). In addition, the mRNA abundances of both *MAFbx* (Fig. 6*C*) and *MuRF-1* (Fig. 6*C*) increased with 6 and 18 h of MV independent of Trolox administration.

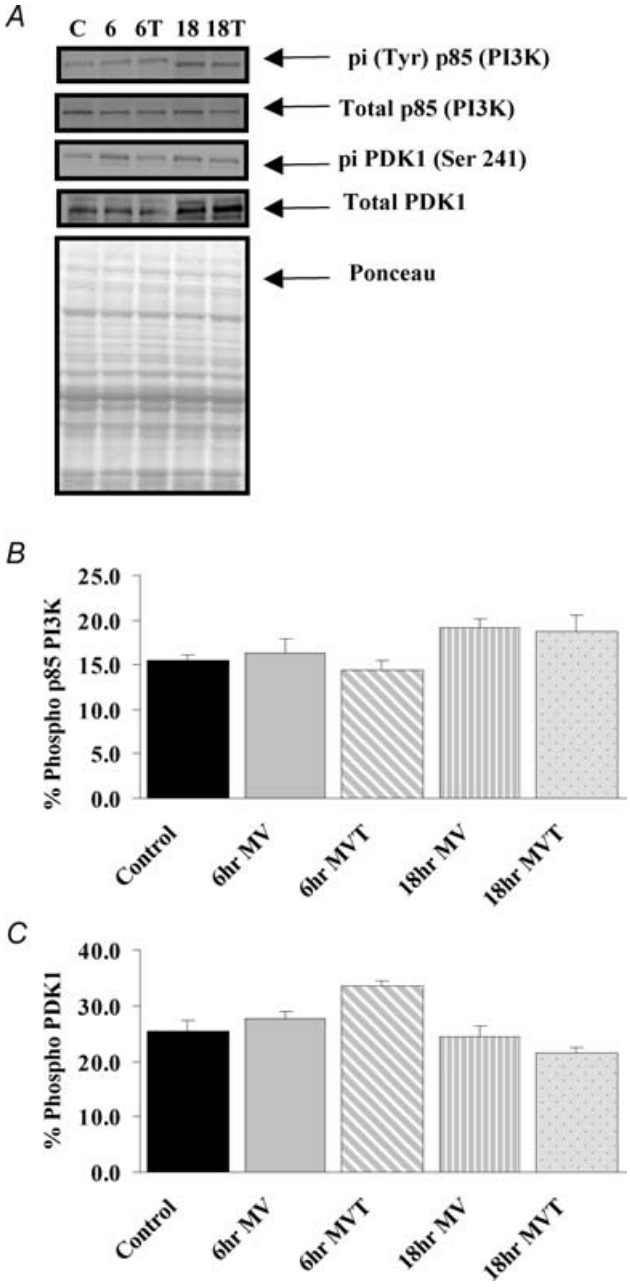

Figure 3. Phosphoinositidyl-3 kinase (PI3K) signalling in diaphragm skeletal muscle with mechanical ventilation
A, representative Western blots and ponceau-stained nitrocellulose membranes to demonstrate even loading and transfer for the analysis of tyrosine (Tyr) phosphorylated p85 PI3K, total PI3K protein, phosphorylated PDK1 (Ser-241), and total PDK1 protein expression. *B*, percentage total cytosolic phosphorylated (% phospho) p85 PI3K protein. *C*, percentage total cytosolic phosphorylated (% phospho) PDK1 protein. Values are percentages of total phosphorylated protein abundance and presented as means ± S.E.M.

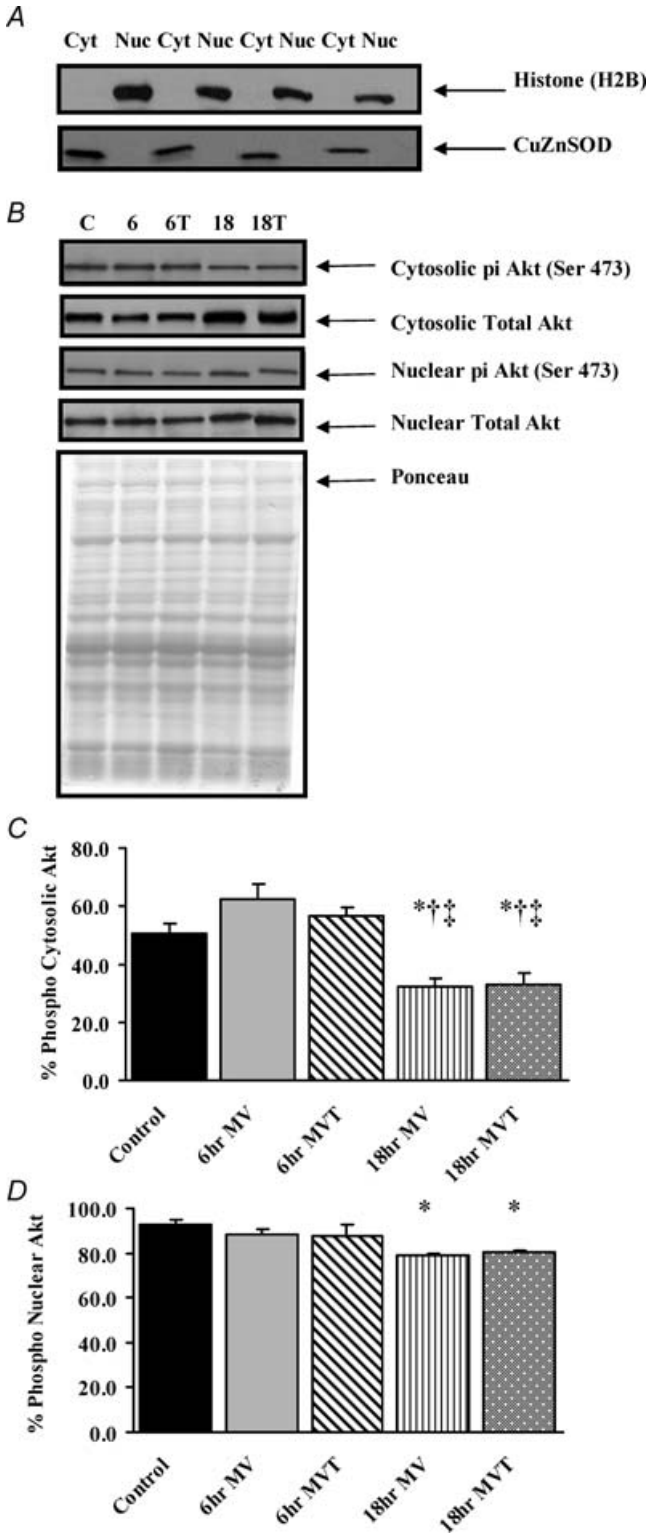

Figure 4. Cytosolic and nuclear compartmentalization of Akt in diaphragm skeletal muscle with mechanical ventilation
A, cellular fractionation of proteins. Whole skeletal muscle homogenates were fractionated into cytosolic and nuclear proteins for Western blot analysis. Representative Western blot of nuclear histone proteins for verification of cellular fractionation. Cytosolic (Cyt) and nuclear (Nuc) protein fractions were subjected to electrophoresis, transferred to nitrocellulose membranes and subsequently probed for expression of the nuclear compartmentalized histone protein 1 (H2B) or the cytosolic compartmentalized copper zinc superoxide dismutase (CuZnSOD) protein. *B*, representative Western blot and ponceau-stained nitrocellulose membranes to demonstrate even loading and transfer for the analysis of Akt in the cytosolic and nuclear compartments of skeletal muscle. *C*, percentage total cytosolic phosphorylated (% phospho) Akt protein. *D*, percentage total nuclear phosphorylated (% phospho) Akt protein. Values are percentages of total phosphorylated protein abundance and presented as means ± S.E.M. * Significantly ($P < 0.05$) different from control values. † Significantly ($P < 0.05$) different from 6 h MV values. ‡ Significantly ($P < 0.05$) different from 6 h MVT values.

Discussion

Overview of principal findings

Our previous work indicates that diaphragmatic atrophy and contractile dysfunction occur within as little as 12 h of MV and are exacerbated during longer periods of MV (Shanely *et al.* 2004; McClung *et al.* 2007). Importantly, alleviation of MV-induced oxidative stress with exogenous antioxidant administration attenuates MV-induced diaphragmatic proteolysis and contractile dysfunction (Betters *et al.* 2004). Nonetheless, the signalling pathways responsible for oxidative stress-induced muscle atrophy and contractile dysfunction remain unknown. To investigate this issue, these experiments tested the hypothesis that oxidative stress down-regulates insulin-like growth factor-1–phosphotidylinositol 3-kinase–Akt serine threonine kinase (IGF-1–PI3K–Akt) signalling and activates the forkhead box O (FoxO) class of transcription factors in diaphragm fibres during MV-induced diaphragm inactivity. Our results confirm that oxidative stress is a critical mechanism for the rapid diaphragm myofibre atrophy during MV. Importantly, these experiments reveal that a down-regulation of IGF-1–PI3K–Akt signalling and up-regulation of FoxO activation and muscle-specific ubiquitin ligase gene expression is an initial event associated with MV-induced diaphragmatic inactivity, occurring at least as early as the onset of oxidative stress during diaphragm disuse (Zergeroglu *et al.* 2003). However, the attenuation of myofibre atrophy by anti-oxidant administration occurs independent of alterations in IGF-1–PI3K–Akt, FoxO activation, or ubiquitin ligase-specific gene expression signalling at both 6 and 18 h time-points of MV. Collectively, these experiments demonstrate for the first time that although oxidative stress plays a limited role in altering IGF-1–PI3K–Akt signalling and FoxO transcription factor activation at 6 and 18 h time-points of MV, it remains necessary for the development of diaphragmatic myofibre atrophy. A detailed discussion of these findings is presented in the following sections.

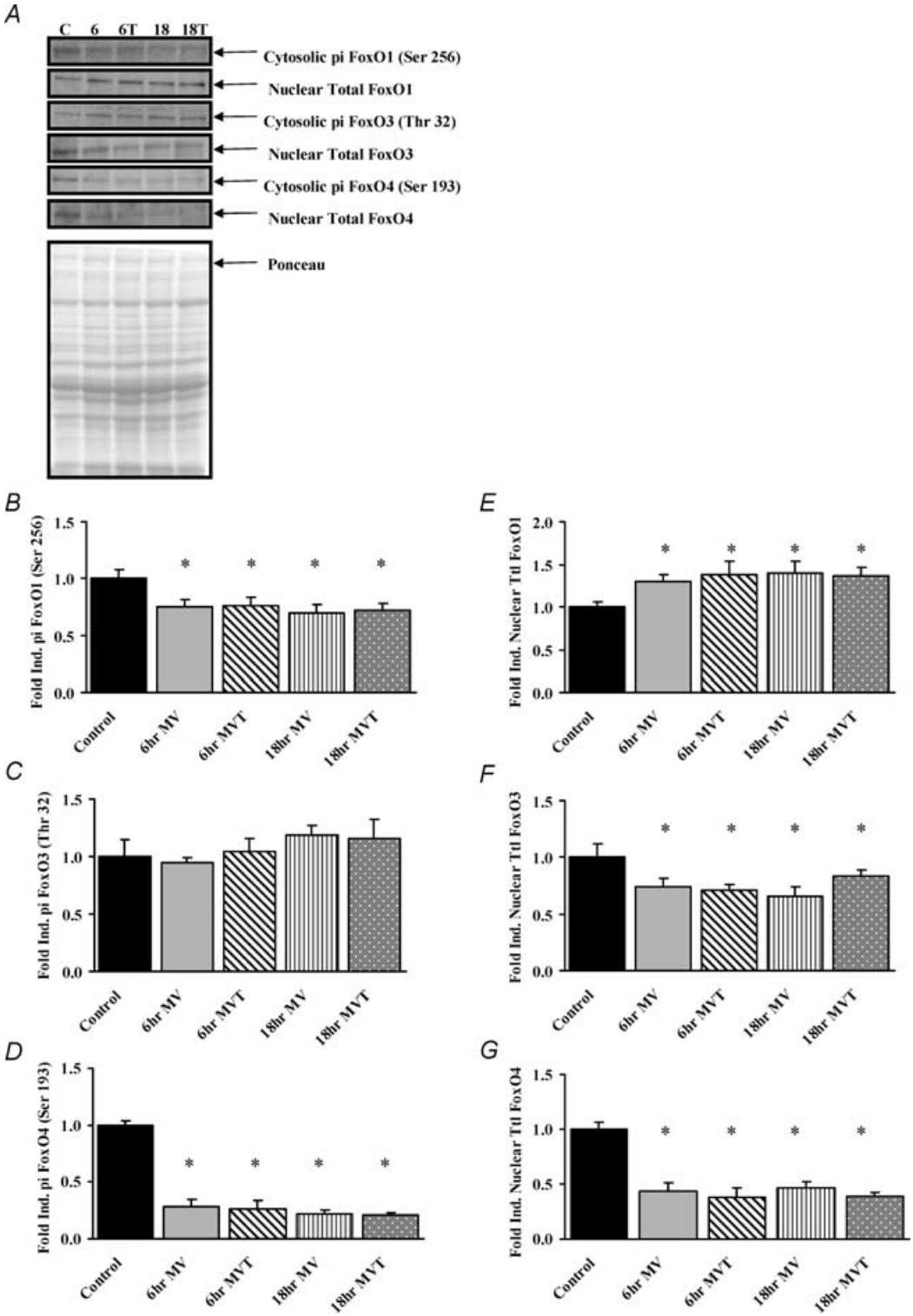

Figure 5. Forkhead transcription factor (FoxO) protein expression in diaphragm skeletal muscle with mechanical ventilation

A, representative Western blot and ponceau-stained nitrocellulose membranes to demonstrate even loading and transfer for the analysis of FoxO1 (Ser-256), phosphorylated FoxO3 (Thr-32), and phosphorylated FoxO4 (Ser-193) and nuclear FoxO1, total FoxO3, and total FoxO4 proteins. *B*, phosphorylated FoxO1 (Ser-256) protein. *C*, phosphorylated FoxO3 (Thr-32) protein expression. *D*, phosphorylated FoxO4 (Ser-256) protein expression. *E*, total nuclear FoxO1 protein expression. *F*, total nuclear FoxO3 protein expression. *G*, total nuclear FoxO4 protein expression. Values are normalized to control values and presented as means ± S.E.M. * Significantly ($P < 0.05$) different from control values.

MV-induced alterations in IGF-1–PI3K–Akt signalling

The current study is the first investigation to examine the impact of diaphragm muscle inactivity due to MV disuse on IGF-1–PI3K–Akt signalling in the diaphragm.

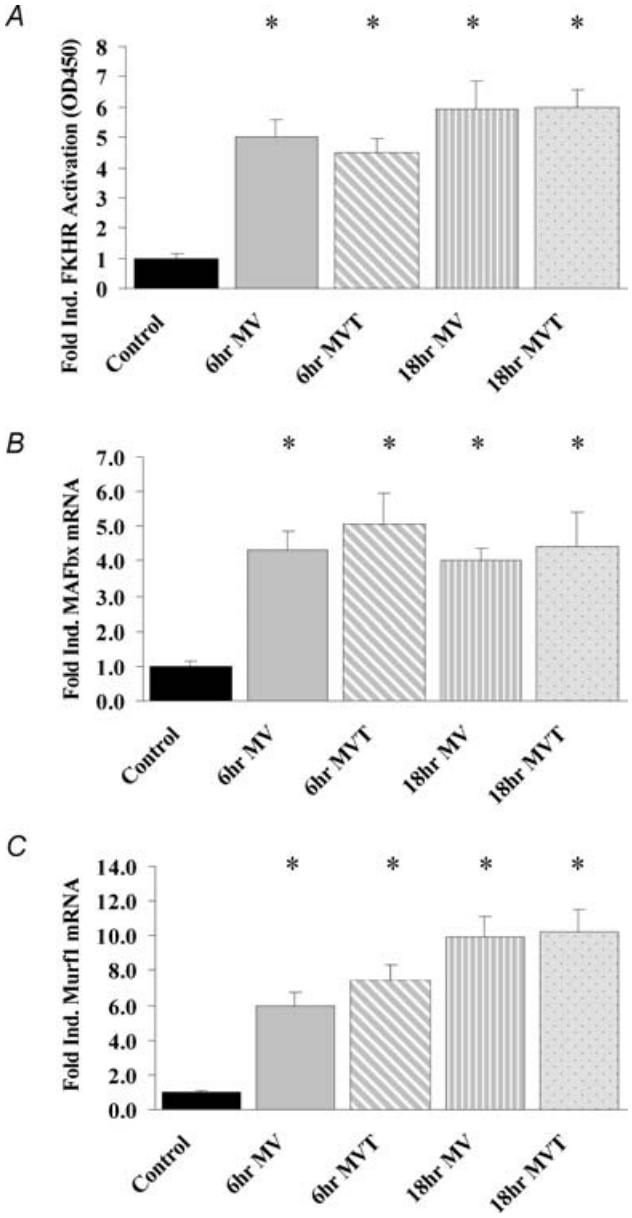

Figure 6. FKHR transcriptional activation and skeletal muscle-specific ubiquitin ligase gene expression in diaphragm skeletal muscle after mechanical ventilation
A, DNA binding of FoxO1. Values are normalized to control values and presented as means ± S.E.M. * Significantly ($P < 0.05$) different from control values. *B*, real-time polymerase chain reaction (RT-PCR) for muscle atrophy transcription factor (*MAFbx*) mRNA abundance. *C*, real-time polymerase chain reaction (RT-PCR) for muscle ring finger-1 (*MuRF-1*) mRNA abundance. Real-time mRNA values are corrected for β-glucuronidase mRNA abundance, normalized to control values and presented as means ± S.E.M. * Significantly ($P < 0.05$) different from control values.

The majority of alterations in diaphragm skeletal muscle IGF-1–PI3K–Akt signalling appear to occur with prolonged ventilation. Down-regulation of signalling components of this pathway, including cytosolic Akt protein, occurred as hypothesized with 18 h of muscle disuse. It is interesting to note that in the current study there is an apparent shift in phosphorylated Akt from the cytosol to the nucleus. Cytosolic Akt phosphorylation protects cardiac myocytes from ischaemic insult but also induces cardiomyocyte hypertrophy and/or cardiomyopathy (Shiraishi *et al.* 2004). Nuclear targeting of activated Akt provides the same cardioprotective functions in ischaemic myocytes devoid of cardiomyopathy (Shiraishi *et al.* 2004). These facts suggest that although activated Akt may function in cytosolic signal propogation, nuclear Akt may serve a specific role in cellular homeostatic transcriptional control in response to varying stimuli. Outside of the aforementioned phosphorylation and deactivation of FoxO proteins in the nucleus, specific nuclear targets of Akt are not well defined. One particular target of interest to the current model is the transcriptional coactivator p300 (Huang & Chen, 2005). This protein interacts with and regulates the transcriptional activity of p53, a proapoptotic transcriptional regulator (Goodman & Smolik, 2000). Myonuclear apoptosis occurs during MV-induced inactivity, and the inhibition of myonuclear loss attenuates myofibre atrophy in this model (McClung *et al.* 2007), suggesting a potential link between nuclear Akt and transcriptional regulation of inactivity induced gene expression. Future work will focus on the possible targets of nuclear activated Akt during MV induced atrophy.

MV-induced alterations in FoxO activation

Activation of skeletal muscle FoxO proteins involves both de-phosphorylation and de-acetylation processes in the cytosol (Stitt *et al.* 2004; Kobayashi *et al.* 2005). As we hypothesized, both 6 and 18 h MV were sufficient to decrease the activity of Akt and increase both the nuclear localization and transcriptional activation of FoxO1 and ubiquitin ligase gene expression. Nuclear exclusion of FoxO proteins by Akt is critical, but not the sole factor in determining their activity (Tsai *et al.* 2003). Our data suggest the maintenance of FoxO transcriptional activity and de-phosphorylation state independent of alterations in upstream repressive influences of IGF-1 signalling. Because 18 h represents a period of time during MV characterized by rapid atrophy development, oxidative damage, and further decreasing levels of protein synthesis in the diaphragm, it is possible that repressive influences of IGF-1 signalling are insufficient to overcome magnified catabolic influences in the diaphragm during MV.

An important and novel finding in the current study is the differential response of FoxO subtypes (FoxO1,

FoxO3 and FoxO4) to mechanical ventilation disuse atrophy. Although FoxO1 protein abundance increased in the nucleus, nuclear FoxO3 and FoxO4 protein abundance decreased during disuse. These facts suggest potential differential roles and/or regulation of individual FoxO proteins during disuse atrophy. FoxO1 and FoxO3 are believed to be predominantly responsible for the induction of muscle-specific ubiquitin ligases during disuse (reviewed in Kandarian & Jackman, 2006). The finding that nuclear FoxO3 decreased independent of alterations in cytosolic FoxO3 may indicate proteolytic degradation of this protein in the diaphragm during MV-induced disuse. Similarly, decreases in both the phosphorylation of cytosolic FoxO4 and total nuclear FoxO4 protein support the potential of decreasing total amounts of this protein during disuse. It is interesting to note that the pattern of FoxO3 and FoxO4 protein loss occurs at a time when FoxO1 is increasingly found in the nucleus and transcriptionally activated. These facts may suggest that IGF-1–Akt's influence on the transcriptional activity of FoxO proteins is regulated specifically by the type of catabolic influence applied and specific to a particular subtype of FoxO protein. Another possibility for consideration is that saturation of promoter regions within genes responsive to FoxO transcription factors results in the selective degradation of non-transcriptionally active FoxO proteins with lesser binding affinities. Future work will focus on both the specificity of activation of different FoxO isoforms between different models of disuse and the potential for competitive DNA binding between different FoxO isoforms.

Oxidative stress and diaphragm myofibre atrophy

We have previously reported that Trolox administration does not attenuate total thiol or alter total glutathione concentrations in the diaphragm of mechanically ventilated rats (Betters *et al.* 2004). Decreasing levels of glutathione often results in increased lipid peroxidation and/or protein carbonyl formation. Biochemical measurement of glutathione alone, however, may not solely be indicative of Trolox-induced protection against diaphragm oxidative stress. The current study did not account for the ratio of total (GSH) to reduced (GSSG) glutathione, which may provide more insight into alterations in antioxidant status during MV. In addition, previous studies similarly demonstrate the inability of Trolox administration to return glutathione values to control levels in ischaemic/reperfused renal cells (Wongmekiat *et al.* 2007). In the current study, despite a lack of alterations in glutathione concentration, Trolox attenuated protein carbonyl formation, indicating the efficacy of this antioxidant in the prevention of oxidative stress-induced skeletal muscle damage.

Recently, Servais *et al.* (2007) demonstrated a protective effect of vitamin E against the development of soleus muscle atrophy during hindlimb unloading. Interestingly, vitamin E administration also attenuated the induction of caspases, calpains and the muscle-specific ubiquitin ligases *MuRF-1* and *MAFbx* during suspension disuse, leading the authors to suggest that the protective effects of vitamin E might be due primarily to modulation of proteolytic genes rather than its antioxidant capabilities. Accordingly, we have previously shown that Trolox administration attenuates *in vitro* protein degradation and 20S proteasome activity in the diaphragm during MV (Betters *et al.* 2004). These facts led us to hypothesize that alterations in Akt–FoxO regulation of ubiquitin ligase gene expression could be a mechanism for the protective effects of antioxidant therapy against disuse-induced muscle atrophy. Results of the current experiments, however, suggest that oxidative stress may serve as an accelerant to skeletal muscle disuse atrophy independent of Akt–FoxO signalling or gene expression of muscle-specific E3 ligases. The rapidity of MV-induced diaphragm myofibre atrophy, however, greatly exceeds the time course of atrophy observed in locomotor muscles during periods of disuse (Adams *et al.* 2003; McClung *et al.* 2007). This observation suggests that MV-induced atrophic signalling may involve different and/or accelerated mechanisms as compared to other models of disuse. In this regard, oxidative injury in the diaphragm occurs within the first 6 h of exposure to MV (Zergeroglu *et al.* 2003). In comparison to locomotor skeletal muscles, disuse-induced oxidative stress (e.g. immobilization or hindlimb suspension) first appears following ∼96 h of unloading (Kondo *et al.* 1992, 1993; Stevenson *et al.* 2003). This is significant because growing evidence implicates oxidative stress as a critical signalling component and potential accelerant of the rapid atrophic development in this model (Powers *et al.* 2007).

The alleviation of oxidative stress may attenuate disuse atrophy through a variety of mechanisms, including alterations in regulatory mechanisms for proteolysis. The possibility exists that the antioxidant-induced suppression of atrophic development in the diaphragm during MV may be due to the protease activity of skeletal muscle calpains and caspases. Myofilament proteins are more resistant to proteolysis when bound to the sarcomeric architecture, therefore actin and myosin must be cleaved to undergo proteolysis at the hands of the proteasome (Powers *et al.* 2005). Activation of calpain and/or caspase skeletal muscle proteases results in cleavage of titin and nebulin sarcomeric proteins from their architectural lattice and allows the proteasome access to actin/myosin proteins for proteolysis (reviewed in Powers *et al.* 2005, 2007). Recently, activation of caspase-3 was determined to be a critical factor in the progression of contractile dysfunction and atrophy induced by both sepsis (Supinski & Callahan, 2006) and MV (McClung *et al.* 2007). Furthermore, the

activation of calpain and caspase proteases is free-radical dependent in numerous cell types (Supinski & Callahan, 2007). The attenuation of oxidative stress-induced calpain- and/or caspase-mediated cleavage of structural sarcomeric proteins with antioxidant therapy provides a potential mechanism for the alleviation of atrophy and contractile dysfunction independent of intracellular signalling to FoxO transcription factors during MV disuse. Future work will explore the signalling mechanisms potentially linking the catabolic influence of oxidative stress to myofilament cleavage during diaphragmatic disuse.

Conclusion

In conclusion, our data reveal that the alleviation of oxidative injury to the diaphragm with the antioxidant Trolox attenuates atrophy induced by MV independent of Akt's influence on FoxO transcription of *MAFbx* and *MuRF-1* ubiquitin ligases at both 6 and 18 h of MV. Our results also demonstrate that there is a time-dependent differential activation of PI3K–Akt signalling proteins during skeletal muscle disuse. Given that muscle wasting due to disuse or disease is a significant clinical problem in both postural and respiratory skeletal muscle, it is important to develop therapeutic countermeasures to retard atrophy and weakness. In this regard, the current basic investigation provides a theoretical basis for future translational clinical studies investigating therapeutic countermeasures to retard inactivity-induced skeletal muscle atrophy and dysfunction in the diaphragm.

References

Adams GR, Caiozzo VJ & Baldwin KM (2003). Skeletal muscle unweighting: spaceflight and ground-based models. *J Appl Physiol* **95**, 2185–2201.

Ausoni S, Gorza L, Schiaffino S, Gundersen K & Lomo T (1990). Expression of myosin heavy chain isoforms in stimulated fast and slow rat muscles. *J Neurosci* **10**, 153–160.

Betters JL, Criswell DS, Shanely RA, Van Gammeren D, Falk D, Deruisseau KC, Deering M, Yimlamai T & Powers SK (2004). Trolox attenuates mechanical ventilation-induced diaphragmatic dysfunction and proteolysis. *Am J Respir Crit Care Med* **170**, 1179–1184.

Bizzozero OA, Reyes S, Ziegler J & Smerjac S (2007). Lipid peroxidation scavengers prevent the carbonylation of cytoskeletal brain proteins induced by glutathione depletion. *Neurochem Res* (in press); DOI: 10.1007/s11064-007-9377-y

Bodine SC, Latres E, Baumhueter S, Lai VK, Nunez L, Clarke BA, Poueymirou WT, Panaro FJ, Na E, Dharmarajan K, Pan ZQ, Valenzuela DM, DeChiara TM, Stitt TN, Yancopoulos GD & Glass DJ (2001). Identification of ubiquitin ligases required for skeletal muscle atrophy. *Science* **294**, 1704–1708.

Criswell DS, Shanely RA, Betters JJ, McKenzie MJ, Sellman JE, Van Gammeren DL & Powers SK (2003). Cumulative effects of aging and mechanical ventilation on *in vitro* diaphragm function. *Chest* **124**, 2302–2308.

DeRuisseau KC, Kavazis AN, Deering MA, Falk DJ, Van Gammeren D, Yimlamai T, Ordway GA & Powers SK (2005*a*). Mechanical ventilation induces alterations of the ubiquitin-proteasome pathway in the diaphragm. *J Appl Physiol* **98**, 1314–1321.

DeRuisseau KC, Kavazis AN & Powers SK (2005*b*). Selective downregulation of ubiquitin conjugation cascade mRNA occurs in the senescent rat soleus muscle. *Exp Gerontol* **40**, 526–531.

DeRuisseau KC, Shanely RA, Akunuri N, Hamilton MT, Van Gammeren D, Zergeroglu AM, McKenzie M & Powers SK (2005*c*). Diaphragm unloading via controlled mechanical ventilation alters the gene expression profile. *Am J Respir Crit Care Med* **172**, 1267–1275.

Furukawa-Hibi Y, Kobayashi Y, Chen C & Motoyama N (2005). FOXO transcription factors in cell-cycle regulation and the response to oxidative stress. *Antioxid Redox Signal* **7**, 752–760.

Gayan-Ramirez G, De Paepe K, Cadot P & Decramer M (2003). Detrimental effects of short-term mechanical ventilation on diaphragm function and IGF-I mRNA in rats. *Intensive Care Med* **29**, 825–833.

Glass DJ (2005). Skeletal muscle hypertrophy and atrophy signaling pathways. *Int J Biochem Cell Biol* **37**, 1974–1984.

Goodman RH & Smolik S (2000). CBP/p300 in cell growth, transformation, and development. *Genes Dev* **14**, 1553–1577.

Huang WC & Chen CC (2005). Akt phosphorylation of p300 at Ser-1834 is essential for its histone acetyltransferase and transcriptional activity. *Mol Cell Biol* **25**, 6592–6602.

Jergovic D, Stal P, Lidman D, Lindvall B & Hildebrand C (2001). Changes in a rat facial muscle after facial nerve injury and repair. *Muscle Nerve* **24**, 1202–1212.

Kandarian SC & Jackman RW (2006). Intracellular signaling during skeletal muscle atrophy. *Muscle Nerve* **33**, 155–165.

Kandarian SC & Stevenson EJ (2002). Molecular events in skeletal muscle during disuse atrophy. *Exerc Sport Sci Rev* **30**, 111–116.

Kobayashi Y, Furukawa-Hibi Y, Chen C, Horio Y, Isobe K, Ikeda K & Motoyama N (2005). SIRT1 is critical regulator of FOXO-mediated transcription in response to oxidative stress. *Int J Mol Med* **16**, 237–243.

Kondo H, Miura M, Nakagaki I, Sasaki S & Itokawa Y (1992). Trace element movement and oxidative stress in skeletal muscle atrophied by immobilization. *Am J Physiol Endocrinol Metab* **262**, E583–E590.

Kondo H, Nakagaki I, Sasaki S, Hori S & Itokawa Y (1993). Mechanism of oxidative stress in skeletal muscle atrophied by immobilization. *Am J Physiol Endocrinol Metab* **265**, E839–E844.

Latres E, Amini AR, Amini AA, Griffiths J, Martin FJ, Wei Y, Lin HC, Yancopoulos GD & Glass DJ (2005). Insulin-like growth factor-1 (IGF-1) inversely regulates atrophy-induced genes via the phosphatidylinositol 3-kinase/Akt/mammalian target of rapamycin (PI3K/Akt/mTOR) pathway. *J Biol Chem* **280**, 2737–2744.

Le Bourdelles G, Viires N, Boczkowski J, Seta N, Pavlovic D & Aubier M (1994). Effects of mechanical ventilation on diaphragmatic contractile properties in rats. *Am J Respir Crit Care Med* **149**, 1539–1544.

Levine S, Nguyen T, Friscia M, Kaiser LR & Shrager JB (2006). Ventilator-induced atrophy in human diaphragm myofibers. *Proc Am Thorac Soc* **3**, A27.

McClung JM, Kavazis AN, Deruisseau KC, Falk DJ, Deering MA, Lee Y, Sugiura T & Powers SK (2007). Caspase-3 regulation of diaphragm myonuclear domain during mechanical ventilation-induced atrophy. *Am J Respir Crit Care Med* **175**, 150–159.

Matsuzaki H, Daitoku H, Hatta M, Tanaka K & Fukamizu A (2003). Insulin-induced phosphorylation of FKHR (Foxo1) targets to proteasomal degradation. *Proc Natl Acad Sci U S A* **100**, 11285–11290.

Powers SK, Kavazis AN & DeRuisseau KC (2005). Mechanisms of disuse muscle atrophy: role of oxidative stress. *Am J Physiol Regul Integr Comp Physiol* **288**, R337–R344.

Powers SK, Kavazis AN & McClung JM (2007). Oxidative stress and disuse muscle atrophy. *J Appl Physiol* **102**, 2389–2397.

Powers SK, Shanely RA, Coombes JS, Koesterer TJ, McKenzie M, Van Gammeren D, Cicale M & Dodd SL (2002). Mechanical ventilation results in progressive contractile dysfunction in the diaphragm. *J Appl Physiol* **92**, 1851–1858.

Sagach VF, Scrosati M, Fielding J, Rossoni G, Galli C & Visioli F (2002). The water-soluble vitamin E analogue Trolox protects against ischaemia/reperfusion damage *in vitro* and *ex vivo*. A comparison with vitamin E. *Pharmacol Res* **45**, 435–439.

Sandri M, Sandri C, Gilbert A, Skurk C, Calabria E, Picard A, Walsh K, Schiaffino S, Lecker SH & Goldberg AL (2004). Foxo transcription factors induce the atrophy-related ubiquitin ligase atrogin-1 and cause skeletal muscle atrophy. *Cell* **117**, 399–412.

Servais S, Letexier D, Favier R, Duchamp C & Desplanches D (2007). Prevention of unloading-induced atrophy by vitamin E supplementation: Links between oxidative stress and soleus muscle proteolysis? *Free Radic Biol Med* **42**, 627–635.

Shanely RA, Van Gammeren D, DeRuisseau KC, Zergeroglu AM, McKenzie MJ, Yarasheski KE & Powers SK (2004). Mechanical ventilation depresses protein synthesis in the rat diaphragm. *Am J Respir Crit Care Med* **170**, 994–999.

Shanely RA, Zergeroglu MA, Lennon SL, Sugiura T, Yimlamai T, Enns D, Belcastro A & Powers SK (2003). Protein synthesis and myosin heavy chain mRNA in the rat diaphragm during mechanical ventilation. *FASEB J* **17**, A435.

Shanely RA, Zergeroglu MA, Lennon SL, Sugiura T, Yimlamai T, Enns D, Belcastro A & Powers SK (2002). Mechanical ventilation-induced diaphragmatic atrophy is associated with oxidative injury and increased proteolytic activity. *Am J Respir Crit Care Med* **166**, 1369–1374.

Shiraishi I, Melendez J, Ahn Y, Skavdahl M, Murphy E, Welch S, Schaefer E, Walsh K, Rosenzweig A, Torella D, Nurzynska D, Kajstura J, Leri A, Anversa P & Sussman MA (2004). Nuclear targeting of Akt enhances kinase activity and survival of cardiomyocytes. *Circ Res* **94**, 884–891.

Siu PM & Alway SE (2005). Mitochondria-associated apoptotic signalling in denervated rat skeletal muscle. *J Physiol* **565**, 309–323.

Stevenson EJ, Giresi PG, Koncarevic A & Kandarian SC (2003). Global analysis of gene expression patterns during disuse atrophy in rat skeletal muscle. *J Physiol* **551**, 33–48.

Stitt TN, Drujan D, Clarke BA, Panaro F, Timofeyva Y, Kline WO, Gonzalez M, Yancopoulos GD & Glass DJ (2004). The IGF-1/PI3K/Akt pathway prevents expression of muscle atrophy-induced ubiquitin ligases by inhibiting FOXO transcription factors. *Mol Cell* **14**, 395–403.

Supinski GS & Callahan LA (2006). Caspase activation contributes to endotoxin-induced diaphragm weakness. *J Appl Physiol* **100**, 1770–1777.

Supinski G & Callahan LA (2007). Free radical-mediated skeletal muscle dysfunction in inflammatory conditions. *J Appl Physiol* **102**, 2056–2063.

Thomason DB, Biggs RB & Booth FW (1989). Protein metabolism and β-myosin heavy-chain mRNA in unweighted soleus muscle. *Am J Physiol Regul Integr Comp Physiol* **257**, R300–R305.

Tsai WC, Bhattacharyya N, Han LY, Hanover JA & Rechler MM (2003). Insulin inhibition of transcription stimulated by the forkhead protein Foxo1 is not solely due to nuclear exclusion. *Endocrinology* **144**, 5615–5622.

Wongmekiat O, Thamprasert K & Lumlertgul D (2007). Renoprotective effect of trolox against ischaemia-reperfusion injury in rats. *Clin Exp Pharmacol Physiol* **34**, 753–759.

Wu TW, Hashimoto N, Wu J, Carey D, Li RK, Mickle DA & Weisel RD (1990). The cytoprotective effect of Trolox demonstrated with three types of human cells. *Biochem Cell Biol* **68**, 1189–1194.

Zergeroglu MA, McKenzie MJ, Shanely RA, Van Gammeren D, DeRuisseau KC & Powers SK (2003). Mechanical ventilation-induced oxidative stress in the diaphragm. *J Appl Physiol* **95**, 1116–1124.

Acknowledgements

This work was supported by a grant from the National Institutes of Health (R01 HL072789) awarded to S. K. Powers. The myosin heavy chain type I (A4.840) antibody developed by Helen M. Blau was obtained from the Developmental Studies Hybridoma Bank developed under the auspices of the NICHD and maintained by The University of Iowa, Department of Biological Sciences, Iowa City, IA 52242, USA. The authors would like to thank Dr Takao Sugiura, Laboratory of Biomechanics and Physiology, Faculty of Liberal Arts, Yamaguchi University, Yamaguchi, Japan for his kind contribution of the MHC type IIa (SC-71, mouse host, immunoglobulin G (IgG) isotype).